FACTA UNIVERSITATIS
Series: **Mechanics, Automatic Control and Robotics** Vol.3, N° 13, 2003, pp. 511 - 532

METHODS FOR SOLVING PROBLEMS OF ELECTROELASTIC PIEZOELECTRIC BODIES WITH DEFECT APPLYING SPATIAL ANALYSIS IN MATLAB

UDC 53.082.73: 539.4.011:551.324.85

Katica (Stevanović) Hedrih, Ljubiša Perić

Faculty of Mechanical Engineering University of Niš,
18000 Niš, Vojvode Tankosića 3/22, e-mail: katica@masfak.ni.ac.yu

Abstract. *In this paper a selective preview of methods applicable to piezoelectric bodies with initial defects under the assumption that they have infinite dimensions is given. Considered is a semi-infinite crack which lies in the interior of the piezoelectric material. Characteristic quantities which affect the process of crack propagation under external mechanical stresses and electrical field polarization are determined. Using different methods, analytical solutions for the problems of piezoelectric materials were obtained for all three modes of crack deformation. Results for a PZT piezoceramic material gained spatial diagrams of state, numerically processed by computer programming in MATLAB, are presented. It is expected that the obtained solutions of such problems in the theory of electroelasticity can be directly used in engineering practice.*

Key words: *Piezoelectric bodies, defect, crack, analytical methods, numerical experiment, stress state, strain state, electric field state, visualization.*

1. INTRODUCTION

Recently, an intensive work is undertaken on application of Linear Elastic Fracture Mechanics (LEFM) in studying piezoelectric materials. Practically, fracture mechanics enables reliable calculation of the lasting period of piezoelements in the design phase already based on mechanical characteristics of the used piezoelectric materials and stresses which occur during exploitation. Also, fracture mechanics can determine reliably the critical error for a crack type, which, once achieved, leads to the fracture of the piezoplate, due to unstable crack propagation.

Spatial analysis of the stress and strain state of the stressed piezoelectric material in the vicinity of the crack tip is performed by linear-elastic fracture mechanics. Different analytical methods used in the papers of *K. Hedrih* and *Lj. Peric* [6, 7, 8, 9] for the study of the stress and strain states of loaded piezoelectric materials will be presented here.

Received December 20, 2002

Some of these methods are: a) spatial analysis of stress and strain state in the loaded piezoelectric material with crack by the method of representing the components (*u, v, w*) of the displacement vector $\vec{s}$ by double infinite series of arbitrary functions, b) analysis of stress and strain state in the piezoelectric material in the vicinity of the crack tip, in case of plane deformation, c) analysis of stress and strain state in the piezoelectric material in the vicinity of the crack tip, in case of material subjected to out-of-plane shear, and d) application of complex variable function in spatial analysis of stress and strain state in the piezoelectric material with crack. The basic theory of the method of complex functions for the solution of elasticity problems is given in the monograph of *Mushelisvili* [13].

A representation of the components (*u, v, w*) of the displacement vector $\vec{s}$ (method-a) by a double infinite series of arbitrary functions was suggested by *Hartranft* and *Sih*, 1969 [5], and later it was further elaborated in 1990 by *H. A. Sosa* and *Y. E. Pak* [19], while the procedures of analysis of crack problem in piezoelectric material quoted under b, c, and d conditions above can be found in references [6-9]. Despite the fact that piezoelectric materials are used for decades in many electromechanic devices, a small number of papers has been published related to their mechanical behavior. From all these papers, the most renowned ones are those of *Parton* (*Fracture mechanics of piezoelectric materials*) [16] and *Deeg* (*The analysis of dislocation, crack, and inclusion problems in piezoelectric solids*) [1] which deal with fracture problems at piezoelectric materials. In 1990 *Pak* obtained a more precise solution for the fracture problem of piezoelectric materials (*Crack extension force in a piezoelectric material*) [14]. In his paper, *Pak* described the behavior of a crack in the interior of a piezoelectric material, as well as, the influence of the piezoelectric material on fracture occurrence. He also proved that crack growth could be accelerated or decelerated depending of the magnitude and the direction of the applied electric field. Research published by *Pak* is in agreement with that of *Deeg* (1980), and concerns the treatment of the problem of fracture of piezoelectric materials by the method of divided dislocation. Related papers are those of *Freiman* (*Mechanical behavior of ferroelectrics ceramics*, 1986) [2] and *Pak* (*Force on a piezoelectric screw dislocation*, 1990) [15].

So far, a great number of experimental papers have been published regarding the strength and toughness of piezoceramic materials which contain faults and defects of different shapes and sizes. The most important are the papers of *W. B. Harrison* et al. (*Monolithic multilayer piezoeletric ceramic transducers,* 1986) [4] and *G.G. Pisarenko* et al. (*Anisotropy of fracture toughness of piezoelectric ceramics*, 1985) [18]. This paper is also based on contents of the monographs on fracture mechanics by *E.E. Gdoutos* [3] and *Krajcinovic – Sumarac* [12].

2. BASIC FORMS OF CRACK DEFORMATION

In fracture mechanics a crack is understood as an absence of cohesive bonds (adhesion) between two adjacent atom layers.

Separated crack surfaces represent boundaries of the stressed body, and therefore stress distribution near the crack tip depends of the form of the fracture surface formation.

There are three basic shapes (modes) of crack deformation (see *E. E. Gdoutos* [3]).

Mode I $K_I \neq 0,\ K_{II} = K_{III} = 0$ **– crack opening**

Mode I of crack deformation (Figure 1) is defined with separation of the fracture surface symmetrically in regard of the primary crack plane: $u = u(r,\varphi),\ v = v(r,\varphi),\ w = 0.$

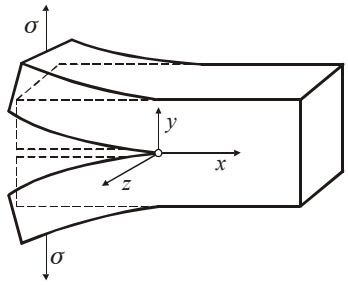

Fig. 1. **Mode I** of crack deformation

Mode II $K_I = 0,\ K_{II} \neq 0,\ K_{III} = 0$ **– shear (slide)**

Mode II of crack deformation (Figure 2) is defined by the movement of one crack surface with respect to the other in the same plane, but in opposite directions: $u = u(r,\varphi),\ v = v(r,\varphi),\ w = 0.$

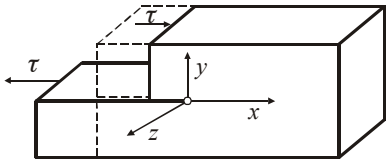

Fig. 2. **Mode II** of crack deformation

Mode III $K_I = 0,\ K_{II} = 0,\ K_{III} \neq 0$ **– shear out of plane**

Mode III of crack deformation (Figure 3) is defined by the movement of one fracture surface along the front of the crack, so that points which were in the same vertical plane before crack growth (development), are allocated on different vertical planes after crack growth: $u = 0,\ v = 0,\ w = w(r,\varphi).$

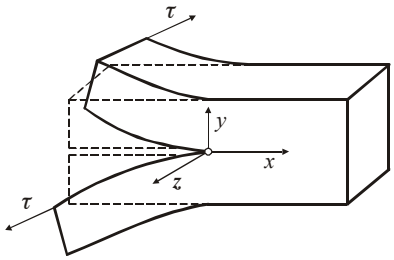

Fig. 3. **Mode III** of crack deformation

Parameters $\boldsymbol{K_I}$, $\boldsymbol{K_{II}}$ and $\boldsymbol{K_{III}}$ are **stress intensity factors** for Mode I, II, and III respectively.

In case of state of plane strain, the front of the crack is an in-plane curve. In an arbitrary point on the curve two modes of crack deformation are present (Mode I and Mode II). Using polar coordinate system (r,φ), the general expressions for components of the tensor of mechanical stress state can be written in the following form:

$$\sigma_{ij}(r,\varphi) = \frac{1}{\sqrt{2\pi r}}[K_I \sigma_{ij}^I(\varphi) + K_{II}\sigma_{ij}^{II}(\varphi)]. \tag{1}$$

In case when the crack front is spatial curve, in an arbitrary point all three modes of crack deformation can be present (Mode I, Mode II, and Mode III). If the observation is performed in polar-cylindrical coordinate system (r,φ,z), general expressions for components of the tensor of mechanical stress state can be written in the following form:

$$\sigma_{ij}(r,\varphi,z) = \frac{1}{\sqrt{2\pi r}}[K_I(z)\sigma_{ij}^I(\varphi) + K_{II}(z)\sigma_{ij}^{II}(\varphi) + K_{III}(z)\sigma_{ij}^{III}(\varphi)]. \tag{2}$$

3. STRESS INTENSITY FACTOR

Linear Elastic Fracture Mechanics (LEFM) is based on the validity of *Hooke*'s law of the material, which contains a crack. However, in the vicinity of the crack tip nonlinear effects dominate, so that the stresses and strains cannot be calculated according to the theory of linear elasticity. For determining of the radius of the plastic area, the most frequently used criteria are those of *Tresca*, *Mises*, *Rosengreen*, *Irwin*, etc. [12, 11, 17].

If the characteristic dimensions of the plastic zone are very small compared to the size of the initial crack and to the dimensions of the specimen, then use of the LEFM in an analysis of stress and strain state in the vicinity of the crack tip is possible. This is justified by the fact that, if the nonlinear area is small, then its influence on the stress distribution at some distance away from the crack tip can be neglected, so that plane elastic solution for the stresses can be used. In that case the **stress intensity factor is a measure of the stress magnitude in the neighborhood of the crack tip**.

The stress intensity factor is defined for a known stress state and geometry. In this case, a fictitious infinite body with a central crack of length $2a$ loaded along three perpendicular directions is introduced. The stress intensity factors are defined as:

$$K_I = \left(\lim_{x\to a^+}\sqrt{2\pi(x-a)}\right)\sigma_y\Big|_{y=0}^{x}, \tag{3}$$

$$K_{II} = \left(\lim_{x\to a^+}\sqrt{2\pi(x-a)}\right)\tau_{xy}\Big|_{y=0}^{x}, \tag{4}$$

$$K_{III} = \left(\lim_{x\to a^+}\sqrt{2\pi(x-a)}\right)\tau_{yz}\Big|_{y=0}^{x}. \tag{5}$$

et consider an infinite plate along the x-y plane of finite thickness, with a central crack of length 2a, stressed in its plane in y-direction (Figure 4), in that case we have: $\sigma_x = 0$, $\sigma_y = \sigma^{\infty}$, $\tau_{xy} = 0$.

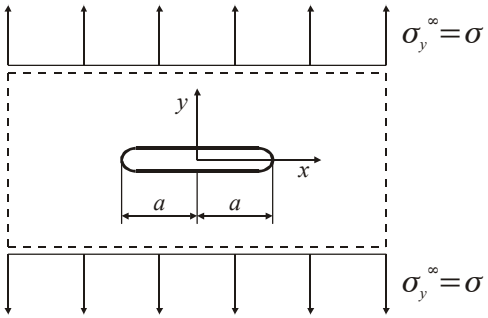

Fig. 4. Infinite plate with central crack

For that problem the *Westergaard*'s solution is known and given by [20]:

$$\sigma_y = \frac{z\sigma}{\sqrt{z^2 - a^2}}, \tag{6}$$

where: $z = x + iy$ – complex variable.

By substitution of expression (6) into expression (3), for y = 0, we obtain:

$$K_I = \lim_{x \to a^+} \sqrt{2\pi(x-a)} \frac{x\sigma}{\sqrt{x^2 - a^2}} = \lim_{x \to a^+} \sqrt{2\pi(x-a)} \frac{x\sigma}{\sqrt{(x-a)(x+a)}} = \sigma\sqrt{\pi a}. \tag{7}$$

In an analogous way, by the described procedure for an infinite plate, we obtain the stress intensity factors for the three modes of crack deformation, also for an infinite plate stressed spatially, which has a central crack of length 2*a* in it:

$$\begin{aligned} K_I &= \sigma\sqrt{\pi a}, \\ K_{II} &= \tau\sqrt{\pi a}, \\ K_{III} &= \tau\sqrt{\pi a}. \end{aligned} \tag{8}$$

Expressions (8) define the stress intensity factors for a central crack loaded at infinity with mechanical stresses σ and τ. Stress intensity factors for characteristic cases which occur most frequently in technical practice, can be found in literature [12, 17].

It can be concluded that, when $r \to 0$ (in the crack tip), stresses become, theoretically, infinitely large, and the stress intensity factor is a measure of the stress field as well as the safety for the stress of destruction at the crack tip.

From expression (8) it can be seen that the dimension of the stress intensity factor $Nm^{-3/2}$. The stress intensity factor *K* is proportional to the stress σ or τ and the square root of the crack length.

4. STARTING EQUATIONS IN POLAR-CYLINDRICAL COORDINATE SYSTEM

For the solution of the problem of mechanical stress and strain distribution in a stressed piezoelectric material, it is necessary to establish relations among the following quantities: tensor of mechanical stress (σ_{ij}), vector of piezoelectric polarization (*electric displacement* - D_i) [17, 19], tensor of strain (ε_{kl}), and vector of electric field magnitude (E_k). The definition of the piezoelectric effect that it occurs through mutual action of mechanical stress and electric field, demands establishing relations between specified states of the coupled fields. This is one of the important tasks of the mechanics of the deformable continua. Experiments are needed to determine the large number of independent material constants in the piezoelectric material.

Equations valid in the spatial theory of LEFM, in absence of volume forces and free electric charges at piezoelectric material, can be written in the following form:

$$H(\varepsilon_{ij}, E_i) = \frac{1}{2} c^E_{ijkl} \varepsilon_{ij} \varepsilon_{kl} - \frac{1}{2} d^{\varepsilon}_{ij} E_i E_j - e_{ikl} \varepsilon_{kl} E_i, \tag{9}$$

$$\varepsilon_{ij} = \frac{1}{2}(u_{i,j} + u_{j,i}), \tag{10}$$

$$\sigma_{ij} = \frac{\partial H}{\partial \varepsilon_{ij}} = c^E_{ijkl} \varepsilon_{kl} - e_{kij} E_k, \tag{11}$$

$$D_i = -\frac{\partial H}{\partial E_i} = e_{ikl} \varepsilon_{kl} + d^{\varepsilon}_{ik} E_k, \tag{12}$$

$$E_i = -\psi_{,i}, \tag{13}$$

$$\sigma_{ij,j} = 0, \tag{14}$$

$$D_{i,i} = 0, \tag{15}$$

where indexes: i, j, k, and l, take values 1, 2, and 3, and other values: σ_{ij}, D_i, ε_{kl}, c_{ijkl}, e_{kij}, d_{ik}, E_k, ψ, are coordinates of tensor, i.e. vector of: mechanical stress, piezoelectric displacement, specific strain, constants of elasticity, piezoconstants, dielectric constants, magnitude of electric field, and electric potential, respectively. Value H, equation (9) represents function of electric enthalpy.

Equation (10) gives a general relation between components of displacement vector $\vec{s}$ and elements of relative strain tensor.

Equation (11) represents extended *Hooke*'s law expressed in tensor form in curvilinear system of coordinates of the mechanical stress, strain and electric field..

Equation (12) is an expression for piezoelectric displacement components, which are also expressed in curvilinear system of coordinates by electric field components and strain.

Equation (13) gives relation between coordinates of electric field and electric potential ψ.

Equations (14) and (15) represent *Navier*'s equations of equilibrium of piezoelectric body for mechanical stresses and equations of equilibrium for componential piezoelectric displacements, respectively.

For a hexagonal crystal system of crystal class 6mm (C_{6v}), generalized *Hooke*'s law (11) has this form:

$$\begin{Bmatrix}\sigma_r\\ \sigma_\varphi\\ \sigma_z\\ \tau_{\varphi z}\\ \tau_{rz}\\ \tau_{r\varphi}\end{Bmatrix}=\begin{bmatrix} c_{11}^E & c_{12}^E & c_{13}^E & 0 & 0 & 0\\ c_{12}^E & c_{11}^E & c_{13}^E & 0 & 0 & 0\\ c_{13}^E & c_{13}^E & c_{33}^E & 0 & 0 & 0\\ 0 & 0 & 0 & c_{44}^E & 0 & 0\\ 0 & 0 & 0 & 0 & c_{44}^E & 0\\ 0 & 0 & 0 & 0 & 0 & \dfrac{c_{11}^E-c_{12}^E}{2}\end{bmatrix}\begin{Bmatrix}\varepsilon_r\\ \varepsilon_\varphi\\ \varepsilon_z\\ 2\varepsilon_{\varphi z}\\ 2\varepsilon_{rz}\\ 2\varepsilon_{r\varphi}\end{Bmatrix}-\begin{bmatrix} 0 & 0 & e_{31}\\ 0 & 0 & e_{31}\\ 0 & 0 & e_{33}\\ 0 & e_{15} & 0\\ e_{15} & 0 & 0\\ 0 & 0 & 0\end{bmatrix}\begin{Bmatrix}E_r\\ E_\varphi\\ E_z\end{Bmatrix}, \tag{16}$$

$$\begin{Bmatrix}D_r\\ D_\varphi\\ D_z\end{Bmatrix}=\begin{bmatrix} 0 & 0 & 0 & 0 & e_{15} & 0\\ 0 & 0 & 0 & e_{15} & 0 & 0\\ e_{31} & e_{31} & e_{33} & 0 & 0 & 0\end{bmatrix}\begin{Bmatrix}\varepsilon_r\\ \varepsilon_\varphi\\ \varepsilon_z\\ 2\varepsilon_{\varphi z}\\ 2\varepsilon_{rz}\\ 2\varepsilon_{r\varphi}\end{Bmatrix}+\begin{bmatrix} d_{11}^\varepsilon & 0 & 0\\ 0 & d_{11}^\varepsilon & 0\\ 0 & 0 & d_{33}^\varepsilon\end{bmatrix}\begin{Bmatrix}E_r\\ E_\varphi\\ E_z\end{Bmatrix}. \tag{17}$$

From matrix relation (16) we get the following expressions for the components mechanical stresses:

$$\begin{aligned}\sigma_r &= c_{11}^E\varepsilon_r + c_{12}^E\varepsilon_\varphi + c_{13}^E\varepsilon_z - e_{31}E_z,\\ \sigma_\varphi &= c_{12}^E\varepsilon_r + c_{11}^E\varepsilon_\varphi + c_{13}^E\varepsilon_z - e_{31}E_z,\\ \sigma_z &= c_{13}^E\varepsilon_r + c_{13}^E\varepsilon_\varphi + c_{33}^E\varepsilon_z - e_{33}E_z,\\ \tau_{\varphi z} &= 2c_{44}^E\varepsilon_{\varphi z} - e_{15}E_\varphi,\\ \tau_{rz} &= 2c_{44}^E\varepsilon_{rz} - e_{15}E_r,\\ \tau_{r\varphi} &= (c_{11}^E - c_{12}^E)\varepsilon_{r\varphi}.\end{aligned} \tag{18}$$

From matrix relation (17) we get the following expressions for the components piezoelectric displacements:

$$\begin{aligned}D_r &= 2e_{15}\varepsilon_{rz} + d_{11}^\varepsilon E_r,\\ D_\varphi &= 2e_{15}\varepsilon_{\varphi z} + d_{11}^\varepsilon E_\varphi,\\ D_z &= e_{31}\varepsilon_r + e_{31}\varepsilon_\varphi + e_{33}\varepsilon_z + d_{33}^\varepsilon E_z.\end{aligned} \tag{19}$$

5. POSTULATE FOR THE PROBLEM OF A SEMI-INFINITE CRACK

Piezoelectric ceramics with a hexagonal crystal system of crystal class 6mm, with infinite dimensions are analyzed. This ceramics has five elastic, three piezoelectric and two dielectric material constants, i.e. altogether ten independent material constants. This kind of piezoelectric material is most often used in ultrasound high power transducers, because it possesses great efficiency of conversion of electric energy into mechanical energy, and vice versa.

Polar-cylindrical system of coordinates r, φ, z, (Figure 5) are used. Limits of polar-cylindrical coordinates are: $0 \le r < \infty$, $-\pi \le \varphi \le \pi$, $-\infty < z < \infty$.

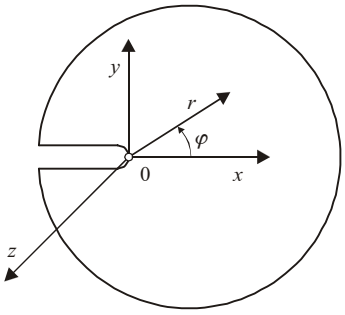

Fig. 5. Semi-infinite crack

For the purpose of easier solving, it is needed to define orientation of the crack (Figure 5). It is assumed that the front of the crack is straight, along the z-axis, while the y-axis is perpendicular on the base plane of the crack. Further, it is assumed that the crack has no surface micro-defects, and that it is not under pressure. The origin of the adopted coordinate system is situated at the tip of the semi-infinite crack. Such configuration and orientation of the crack leads to special interaction between the tensors of mechanical stress and the vector of the electric field, as well as between the vector of the piezoelectric displacements and the tensor of the relative mechanical strain. Examination of other crack orientations and their consequences will not be studied in this paper

On the crack surface, when $\varphi = \pm\pi$, it is assumed that the following components of the mechanical stresses and piezoelectric displacements are equal to zero:

– normal mechanical stress for the surface with normal in circular direction:

$$\sigma_{\varphi} = 0, \tag{20}$$

– shear mechanical stress in radial direction for the surface with normal in circular direction:

$$\tau_{\varphi r} = 0, \tag{21}$$

– shear mechanical stress in axial direction for the surface with normal in circular direction:

$$\tau_{\varphi z} = 0, \tag{22}$$

– piezoelectric displacement in circular direction in the spots of the crack surface:

$$D_{\varphi} = 0. \tag{23}$$

These boundary conditions on the sides of the crack surface were first suggested by *Y.E. Pak*, in 1987 [14]. Thus the problem of the semi-infinite crack in an infinite piezoelectric material was defined.

6. METHOD OF SOLUTION BY DOUBLE INFINITE SERIES OF ARBITRARY FUNCTIONS

The problem of the three-dimensional semi-infinite crack, as defined earlier, is solved by expressing the physical coordinates (u,v,w) of the displacement vector $\vec{s}$, and electric potential $\psi(r,\varphi,z)$, by double infinite series of arbitrary functions (R_n, Φ_n, Z_n, and K_n), i.e.:

$$(u,v,w,\psi) = \sum_{m=0}^{\infty}\sum_{n=0}^{\infty} r^{\lambda_m+n}(R_n,\Phi_n,Z_n,K_n), \tag{24}$$

or in expanded form:

$$\begin{aligned} u(r,\varphi,z) &= \sum_{m=0}^{\infty}\sum_{n=0}^{\infty} r^{\lambda_m+n} R_n(\varphi,z), \\ v(r,\varphi,z) &= \sum_{m=0}^{\infty}\sum_{n=0}^{\infty} r^{\lambda_m+n} \Phi_n(\varphi,z), \\ w(r,\varphi,z) &= \sum_{m=0}^{\infty}\sum_{n=0}^{\infty} r^{\lambda_m+n} Z_n(\varphi,z), \\ \psi(r,\varphi,z) &= \sum_{m=0}^{\infty}\sum_{n=0}^{\infty} r^{\lambda_m+n} K_n(\varphi,z). \end{aligned} \tag{25}$$

The introduced arbitrary functions (R_n, Φ_n, Z_n, and K_n) depend on: polar angle φ, cylindrical coordinate z and eigenvalue λ_m, and they are equal to zero for $n < 0$, because infinite displacements and electric potential in the crack tip are impossible. Eigenvalues λ_m ($m = 0, 1, 2, 3,$) are considered as constants to be determined.

Further procedure of deriving the above quantities for the final solution, is shown in papers [17] and [19].

7. METHOD OF DECOMPOSITION TO PLANE STRAIN AND OUT-OF-PLANE SHEAR STATES

In the solution of problems of LEFM for the general case of the three-dimensional deformable body, substantial mathematical difficulties are encountered. For that reason, in some cases, we switch to plane problems of LEFM. Thus, we will deal with the stress and strain state in a piezoelectric material in the vicinity of the crack tip for the case of plane strain and out-of plane shear.

It is mentioned before (article 2), that the decomposition of any spatial problem, when the crack front is a spatial curve, can be done in three basic, mutually independent forms (modes) of crack deformation (mode I, mode II, mode III) [12, 17].

Under plane strain conditions we obtain the first two basic modes of crack deformation (mode I and mode II)..

The third basic mode of crack deformation is related to the case of out of crack plane shear (mode III).

7.1 Plane strain state

Plane strain state is defined by displacement field:

$$u = u(r,\varphi),\ v = v(r,\varphi),\ w = 0, \tag{26}$$

and by electric field:

$$E_r = 0,\ E_\varphi = 0,\ E_z = E_z(r,\varphi). \tag{27}$$

The solution of the problem is performed by *Maxwell*'s partial differential equation, method of parting variables, and using *Airy*'s stress function. General solution for *Airy*'s stress function $\Phi(r,\varphi)$ in the vicinity of the crack tip is expressed using trigonometric series, and the coefficients that depend on crack shape and load are expressed by stress intensity factors K_I and K_{II} [8, 17].

7.2 Shear out of crack plane

In case of out of plane shear, it is assumed that all in plane displacements are equal to zero, and that only displacements in *z*-direction exist, i.e.:

$$u = 0,\ v = 0,\ w = w(r,\varphi). \tag{28}$$

Introducing the expressions for the components of mechanical and piezoelectric stresses into the modified *Navier*'s equations of equilibrium, we get the differential equations for the problem of out of crack plane shear:

$$\begin{aligned} \Delta w &= 0, \\ \Delta\psi &= 0. \end{aligned} \tag{29}$$

The boundary conditions on the crack surfaces are given by mechanical stresses and piezoelectric displacements:

– that shear stress in axial direction for the surface with normal in circular direction is equal to zero:

$$\tau_{\varphi z}(r,\pm\pi) = 0, \tag{30}$$

– that normal piezoelectric displacement for the surface with normal in circular direction is equal to zero:

$$D_\varphi = 0, \tag{31}$$

The unknown constants, that depend on the crack shape and applied load, are expressed by stress intensity factor K_{III}. A more detailed derivation can be found in papers [9] and [17].

8. METHOD OF APPLICATION OF COMPLEX VARIABLE FUNCTION

In this part of the paper, a spatial analysis of the stress and strain state in the vicinity of the crack tip of the stressed piezoelectric material is performed using analytical functions of complex variable (analytical complex functions), expressed in polar coordinates (r, φ). These functions are assumed in the form of infinite exponential series (*Laurent*'s series). The problem is to determine analytical solutions of the stress and strain states, for n-members of the series, when $n \to \infty$ [10, 13].

As in the previous analysis, decomposition of the spatial problem into the three basic, mutually independent modes of crack deformation (mode I, mode II and mode III) is first performed. Each of these modes is then treated separately.

8.1 Plane strain state

In solving problems of plane theory of elasticity, the normal and tangential components of the stress tensor, can be expressed by *Airy*'s stress function $\Phi(r,\varphi)$. When volume forces are absent, the stress function satisfies the *Maxwell* biharmonic partial differential equation [10].

For the application of the method of complex variable function, we express the stress function by analytical functions of complex variable, and then we define the components of the displacement vector and stresses, which satisfy the boundary conditions on the crack surfaces.

By decomposition of the state of plane strain one gets two basic modes of crack deformation: mode I – crack opening (Figure 1.) and mode II – shear (Figure 2.).

8.1.1. Application of the complex variable function

The stress function $\Phi(r,\varphi)$ is defined by two analytical functions $F(z)$ and $\chi(z)$ of the complex variable $z = r\ e^{i\varphi}$ [3, 10]. The normal and shear stresses as well as the displacement vector are expressed by the stress function in polar coordinates as:

$$\frac{\partial\Phi}{\partial r}+i\frac{1}{r}\frac{\partial\Phi}{\partial\varphi}=\frac{\partial\Phi}{\partial z}\frac{\partial z}{\partial r}+\frac{\partial\Phi}{\partial\bar{z}}\frac{\partial\bar{z}}{\partial r}+i\frac{\partial\Phi}{\partial z}\frac{1}{r}\frac{\partial z}{\partial\varphi}+i\frac{\partial\Phi}{\partial\bar{z}}\frac{1}{r}\frac{\partial\bar{z}}{\partial\varphi}=2\frac{\partial\Phi}{\partial\bar{z}}e^{-i\varphi}. \tag{32}$$

Relation between stress function $\Phi(r,\varphi)$ and complex function $F(z)$ can be found in literature [10] and [17], in the form of:

$$\Phi(r,\varphi)=\mathrm{Re}\{\bar{z}F(z)+\chi(z)\}=\frac{1}{2}[\bar{z}F(z)+z\overline{F}(\bar{z})+\chi(z)+\overline{\chi}(\bar{z})], \tag{33}$$

A more detailed derivation, of the final solution, can be seen in literature [6], [7] and [17].

8.2 Shear of material out of crack plane

Mode III of crack deformation is shown in Figure 3. Out –of –plane shear of the material is characterized by the displacement along the direction of the z-axis i.e., $w = w(r, \varphi)$, while the other two displacements ($u = 0$, $v = 0$) are zero.

8.2.1. Stress and strain state for Mode III

The complex functions $W(z)$ and $\Phi(z)$, which are used in analysis of the stress and strain state in case of out of crack plane shear (mode III) have a form of a series:

$$\begin{aligned} W(z)&=\sum_{n=0}^{\infty}\left[E_{2n}\,\mathrm{Re}(z^n)+E_{2n+1}\,\mathrm{Im}\left(z^{\frac{2n+1}{2}}\right)\right]= \\ &=E_0+E_1\,\mathrm{Im}\left(z^{\frac{1}{2}}\right)+E_2\,\mathrm{Re}(z)+E_3\,\mathrm{Im}\left(z^{\frac{3}{2}}\right)+\ldots, \end{aligned} \tag{34}$$

$$\Phi(z)=\sum_{n=0}^{\infty}\left[F_{2n}\,\mathrm{Re}(z^n)+F_{2n+1}\,\mathrm{Im}\left(z^{\frac{2n+1}{2}}\right)\right]= \\ =F_0+F_1\,\mathrm{Im}\left(z^{\frac{1}{2}}\right)+F_2\,\mathrm{Re}(z)+F_3\,\mathrm{Im}\left(z^{\frac{3}{2}}\right)+\ldots, \tag{35}$$

where $z = re^{i\varphi}$ is complex variable.

Further details to determine the components of displacement w, the electric potential ψ, the components of strain tensor, the components of mechanical stress tensor, the components of the vector of piezoelectric displacement, the components of the vector of the electric field can be found in references [6], [7] and [17].

9. REVIEW OF DERIVED EQUATIONS – SOLUTIONS

A general characteristic of all described methods is that they lead to identical general solutions for a specific number of series members. The most general method is that of applying the complex variable function (article 8), whose solutions can be shown for all three modes of crack deformation individually [6], [7] and [17] as:

Mod I

$$\sigma_r=\frac{1}{2}\sum_{n=0}^{\infty}nr^{\frac{n}{2}-1}\left[\left(3-\frac{n}{2}\right)A_n\cos\left(\frac{n}{2}-1\right)\varphi-B_n\cos\left(\frac{n}{2}+1\right)\varphi\right], \tag{36}$$

$$\sigma_\varphi=\frac{1}{2}\sum_{n=0}^{\infty}nr^{\frac{n}{2}-1}\left[\left(\frac{n}{2}+1\right)A_n\cos\left(\frac{n}{2}-1\right)\varphi+B_n\cos\left(\frac{n}{2}+1\right)\varphi\right], \tag{37}$$

$$\sigma_z=\frac{2c_{13}}{c_{11}+c_{12}}\sum_{n=0}^{\infty}nr^{\frac{n}{2}-1}A_n\cos\left(\frac{n}{2}-1\right)\varphi, \tag{38}$$

$$\tau_{r\varphi}=\frac{1}{2}\sum_{n=0}^{\infty}nr^{\frac{n}{2}-1}\left[\left(\frac{n}{2}-1\right)A_n\sin\left(\frac{n}{2}-1\right)\varphi+B_n\sin\left(\frac{n}{2}+1\right)\varphi\right], \tag{39}$$

$$D_z=\frac{2e_{31}}{c_{11}+c_{12}}\sum_{n=0}^{\infty}nr^{\frac{n}{2}-1}A_n\cos\left(\frac{n}{2}-1\right)\varphi, \tag{40}$$

$$\varepsilon_r=\frac{1}{2(c_{11}-c_{12})}\sum_{n=0}^{\infty}nr^{\frac{n}{2}-1}\left[\frac{(6-n)c_{11}-(2+n)c_{12}}{2(c_{11}+c_{12})}A_n\cos\left(\frac{n}{2}-1\right)\varphi-B_n\cos\left(\frac{n}{2}+1\right)\varphi\right], \tag{41}$$

$$\varepsilon_\varphi=\frac{1}{2(c_{11}-c_{12})}\sum_{n=0}^{\infty}nr^{\frac{n}{2}-1}\left[\frac{(2+n)c_{11}-(6-n)c_{12}}{2(c_{11}+c_{12})}A_n\cos\left(\frac{n}{2}-1\right)\varphi+B_n\cos\left(\frac{n}{2}+1\right)\varphi\right], \tag{42}$$

$$\varepsilon_{r\varphi}=\frac{1}{4(c_{11}-c_{12})}\sum_{n=0}^{\infty}nr^{\frac{n}{2}-1}\left[(n-2)A_n\sin\left(\frac{n}{2}-1\right)\varphi+2B_n\sin\left(\frac{n}{2}+1\right)\varphi\right], \tag{43}$$

$$u=\frac{1}{c_{11}-c_{12}}\sum_{n=0}^{\infty}r^{\frac{n}{2}}\left[\frac{(6-n)c_{11}-(2+n)c_{12}}{2(c_{11}+c_{12})}A_n\cos\left(\frac{n}{2}-1\right)\varphi-B_n\cos\left(\frac{n}{2}+1\right)\varphi\right], \quad (44)$$

$$v=\frac{1}{c_{11}-c_{12}}\sum_{n=0}^{\infty}r^{\frac{n}{2}}\left[\frac{(6+n)c_{11}-(2-n)c_{12}}{2(c_{11}+c_{12})}A_n\sin\left(\frac{n}{2}-1\right)\varphi+B_n\sin\left(\frac{n}{2}+1\right)\varphi\right]. \quad (45)$$

Mod II

$$\sigma_r=\frac{1}{2}\sum_{n=0}^{\infty}nr^{\frac{n}{2}-1}\left[C_n\left(\frac{n}{2}-3\right)\sin\left(\frac{n}{2}-1\right)\varphi+D_n\sin\left(\frac{n}{2}+1\right)\varphi\right], \quad (46)$$

$$\sigma_\varphi=-\frac{1}{2}\sum_{n=0}^{\infty}nr^{\frac{n}{2}-1}\left[\left(1+\frac{n}{2}\right)C_n\sin\left(\frac{n}{2}-1\right)\varphi+2D_n\sin\left(\frac{n}{2}+1\right)\varphi\right], \quad (47)$$

$$\sigma_z=-\frac{2c_{13}}{c_{11}+c_{12}}\sum_{n=0}^{\infty}nr^{\frac{n}{2}-1}C_n\sin\left(\frac{n}{2}-1\right)\varphi, \quad (48)$$

$$\tau_{r\varphi}=\frac{1}{2}\sum_{n=0}^{\infty}nr^{\frac{n}{2}-1}\left[\left(\frac{n}{2}-1\right)C_n\cos\left(\frac{n}{2}-1\right)\varphi+D_n\cos\left(\frac{n}{2}+1\right)\varphi\right], \quad (49)$$

$$D_z=-\frac{2e_{31}}{c_{11}+c_{12}}\sum_{n=0}^{\infty}nr^{\frac{n}{2}-1}C_n\sin\left(\frac{n}{2}-1\right)\varphi, \quad (50)$$

$$\varepsilon_r=\frac{1}{2(c_{11}-c_{12})}\sum_{n=0}^{\infty}nr^{\frac{n}{2}-1}\left[\frac{(n-6)c_{11}+(n+2)c_{12}}{2(c_{11}+c_{12})}C_n\sin\left(\frac{n}{2}-1\right)\varphi+D_n\sin\left(\frac{n}{2}+1\right)\varphi\right], \quad (51)$$

$$\varepsilon_\varphi=\frac{1}{2(c_{11}-c_{12})}\sum_{n=0}^{\infty}nr^{\frac{n}{2}-1}\left[\frac{(6-n)c_{12}-(2+n)c_{11}}{2(c_{11}+c_{12})}C_n\sin\left(\frac{n}{2}-1\right)\varphi-D_n\sin\left(\frac{n}{2}+1\right)\varphi\right], \quad (52)$$

$$\varepsilon_{r\varphi}=\frac{1}{2(c_{11}-c_{12})}\sum_{n=0}^{\infty}nr^{\frac{n}{2}-1}\left[\frac{(6-n)c_{12}-(2+n)c_{11}}{2(c_{11}+c_{12})}C_n\sin\left(\frac{n}{2}-1\right)\varphi-D_n\sin\left(\frac{n}{2}+1\right)\varphi\right], \quad (53)$$

$$u=\frac{1}{2(c_{11}-c_{12})}\sum_{n=0}^{\infty}r^{\frac{n}{2}}\left[\frac{(n-6)c_{11}+(n+2)c_{12}}{c_{11}+c_{12}}C_n\sin\left(\frac{n}{2}-1\right)\varphi+2D_n\sin\left(\frac{n}{2}+1\right)\varphi\right], \quad (54)$$

$$v=\frac{1}{2(c_{11}-c_{12})}\sum_{n=0}^{\infty}r^{\frac{n}{2}}\left[\frac{(n+6)c_{11}+(n-2)c_{12}}{c_{11}+c_{12}}C_n\cos\left(\frac{n}{2}-1\right)\varphi+2D_n\cos\left(\frac{n}{2}+1\right)\varphi\right]. \quad (55)$$

Mod III

$$\tau_{rz}=\frac{1}{2}\sum_{n=0}^{\infty}\left[2n(c_{44}E_{2n}+e_{15}F_{2n})r^{n-1}\cos n\varphi+(2n+1)(c_{44}E_{2n+1}+e_{15}F_{2n+1})r^{\frac{2n-1}{2}}\sin\frac{2n+1}{2}\varphi\right], \quad (56)$$

$$\tau_{rz}=\frac{1}{2}\sum_{n=0}^{\infty}\left[2n(c_{44}E_{2n}+e_{15}F_{2n})r^{n-1}\cos n\varphi+(2n+1)()c_{44}E_{2n+1}+e_{15}F_{2n+1}\,r^{\frac{2n-1}{2}}\sin\frac{2n+1}{2}\varphi\right], \quad (57)$$

$$\tau_{\varphi z}=\frac{1}{2}\sum_{n=0}^{\infty}\left[-2n(c_{44}E_{2n}+e_{15}F_{2n})r^{n-1}\sin n\varphi+(2n+1)(c_{44}E_{2n+1}+e_{15}F_{2n+1})\,r^{\frac{2n-1}{2}}\cos\frac{2n+1}{2}\varphi\right], \quad (58)$$

$$D_{r}=\frac{1}{2}\sum_{n=0}^{\infty}\left[2n(e_{15}E_{2n}-d_{11}F_{2n})r^{n-1}\cos n\varphi+(2n+1)(e_{15}E_{2n+1}-d_{11}F_{2n+1})\,r^{\frac{2n-1}{2}}\sin\frac{2n+1}{2}\varphi\right], \quad (59)$$

$$D_{\varphi}=\frac{1}{2}\sum_{n=0}^{\infty}\left[-2n(e_{15}E_{2n}-d_{11}F_{2n})r^{n-1}\sin n\varphi+(2n+1)(e_{15}E_{2n+1}-d_{11}F_{2n+1})\,r^{\frac{2n-1}{2}}\cos\frac{2n+1}{2}\varphi\right], \quad (60)$$

$$\varepsilon_{rz}=\frac{1}{4}\sum_{n=0}^{\infty}\left[2nE_{2n}r^{n-1}\cos n\varphi+(2n+1)E_{2n+1}r^{\frac{2n-1}{2}}\sin\frac{2n+1}{2}\varphi\right], \quad (61)$$

$$\varepsilon_{\varphi z}=\frac{1}{4}\sum_{n=0}^{\infty}\left[-2nE_{2n}r^{n-1}\sin n\varphi+(2n+1)E_{2n+1}r^{\frac{2n-1}{2}}\cos\frac{2n+1}{2}\varphi\right], \quad (62)$$

$$E_{r}=-\frac{1}{2}\sum_{n=0}^{\infty}\left[2nF_{2n}r^{n-1}\cos n\varphi+(2n+1)F_{2n+1}r^{\frac{2n-1}{2}}\sin\frac{2n+1}{2}\varphi\right], \quad (63)$$

$$E_{\varphi}=-\frac{1}{2}\sum_{n=0}^{\infty}\left[-2nF_{2n}r^{n-1}\sin n\varphi+(2n+1)F_{2n+1}r^{\frac{2n-1}{2}}\cos\frac{2n+1}{2}\varphi\right], \quad (64)$$

$$w(r,\varphi)=\sum_{n=0}^{\infty}\left(E_{2n}r^{n}\cos n\varphi+E_{2n+1}r^{\frac{2n+1}{2}}\sin\frac{2n+1}{2}\varphi\right), \quad (65)$$

$$\psi(r,\varphi)=\sum_{n=0}^{\infty}\left(F_{2n}r^{n}\cos n\varphi+F_{2n+1}r^{\frac{2n+1}{2}}\sin\frac{2n+1}{2}\varphi\right). \quad (66)$$

Coefficients which appear in solutions for: Mode I, Mode II i Mode III (A_n, B_n, C_n, D_n, E_{2n}, F_{2n}, E_{2n+1} *i* F_{2n+1}), equations: (36)÷(66), depend from the crack form, dimensions and shape of the specimen and the external load. They can be expressed by the stress intensity factors K_I, K_{II}, and K_{III} [12, 17].

The crack behavior is studied in a piezoelectric material PZT-4 with density $\rho = 7500\ \mathrm{kg/m^3}$. This material belongs to hexagonal crystal system of crystal class 6mm (C_{6v}), and its material tensors are:

– matrix of elastic constants tensor at constant electric field:

$$[C_{ij}^E]=\begin{bmatrix} c_{11}^E & c_{12}^E & c_{13}^E & 0 & 0 & 0 \\ c_{12}^E & c_{11}^E & c_{13}^E & 0 & 0 & 0 \\ c_{13}^E & c_{13}^E & c_{33}^E & 0 & 0 & 0 \\ 0 & 0 & 0 & c_{44}^E & 0 & 0 \\ 0 & 0 & 0 & 0 & c_{44}^E & 0 \\ 0 & 0 & 0 & 0 & 0 & \dfrac{c_{11}^E - c_{12}^E}{2} \end{bmatrix} = \tag{67}$$

$$= \begin{bmatrix} 13{,}9 & 7{,}78 & 7{,}43 & 0 & 0 & 0 \\ 7{,}78 & 13{,}9 & 7{,}43 & 0 & 0 & 0 \\ 7{,}43 & 7{,}43 & 11{,}5 & 0 & 0 & 0 \\ 0 & 0 & 0 & 2{,}56 & 0 & 0 \\ 0 & 0 & 0 & 0 & 2{,}56 & 0 \\ 0 & 0 & 0 & 0 & 0 & 3{,}06 \end{bmatrix} 10^{10}\left[\frac{N}{m^2}\right],$$

– matrix of piezoconstants tensor:

$$[e_{ij}]=\begin{bmatrix} 0 & 0 & 0 & 0 & e_{15} & 0 \\ 0 & 0 & 0 & e_{15} & 0 & 0 \\ e_{31} & e_{31} & e_{33} & 0 & 0 & 0 \end{bmatrix} = \begin{bmatrix} 0 & 0 & 0 & 0 & 12{,}7 & 0 \\ 0 & 0 & 0 & 12{,}7 & 0 & 0 \\ -5{,}2 & -5{,}2 & 15{,}1 & 0 & 0 & 0 \end{bmatrix} \left[\frac{C}{m^2}\right], \tag{68}$$

– matrix of dielectric constants tensor at given strain:

$$[d_{ij}^{\varepsilon}]=\begin{bmatrix} d_{11}^{\varepsilon} & 0 & 0 \\ 0 & d_{11}^{\varepsilon} & 0 \\ 0 & 0 & d_{33}^{\varepsilon} \end{bmatrix} = \begin{bmatrix} 6{,}46 & 0 & 0 \\ 0 & 6{,}46 & 0 \\ 0 & 0 & 5{,}62 \end{bmatrix} \cdot 10^{-9}\left[\frac{F}{m}\right]. \tag{69}$$

At this time, a numerical analysis of equations (36)÷(66) was performed in MATLAB. The system of equations represents a spatial solution of the crack problem in piezoelectric material. As a result of a numerical analysis in MATLAB one gets spatial diagrams of states, for Mode I, Mode II, and Mode III, of crack deformation of normalized values: $\overline{\sigma}_r, \overline{\sigma}_\varphi, \overline{\sigma}_z, \overline{\tau}_{\varphi r}, \overline{D}_z, \overline{\varepsilon}_r, \overline{\varepsilon}_\varphi, \overline{\varepsilon}_{r\varphi}, \overline{u}, \overline{v}, \overline{\tau}_{rz}, \overline{D}_r, \overline{\varepsilon}_{rz}, \overline{\tau}_{\varphi z}, \overline{D}_\varphi, \overline{\varepsilon}_{\varphi z}, \overline{E}_r, \overline{E}_\varphi, \overline{w}, \overline{\psi}$ (Figs. 6÷31).

Mode I

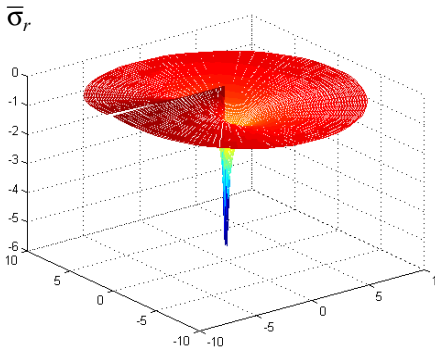

Fig. 6. Mechanical stress $\overline{\sigma}_r = \overline{\sigma}_r(r,\varphi)$

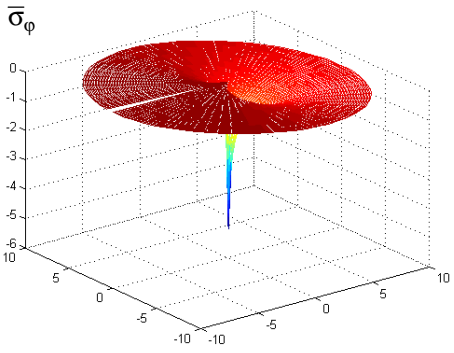

Fig. 7. Mechanical stress $\overline{\sigma}_\varphi = \overline{\sigma}_\varphi(r,\varphi)$

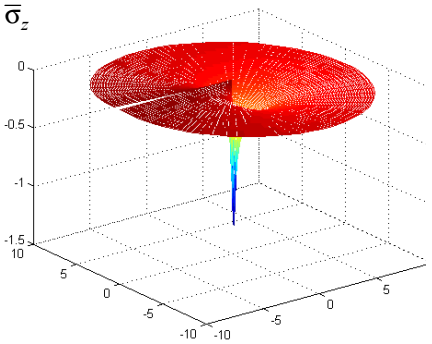

Fig. 8. Mechanical stress $\overline{\sigma}_z = \overline{\sigma}_z(r,\varphi)$

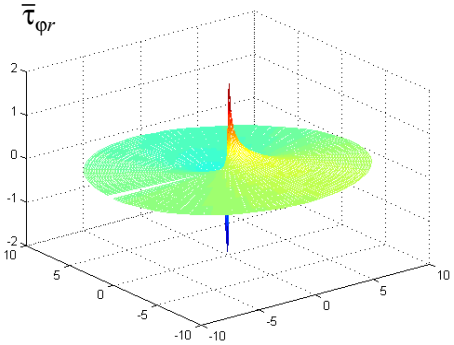

Fig 9. Mechanical stress $\overline{\tau}_{\varphi r} = \overline{\tau}_{\varphi r}(r,\varphi)$

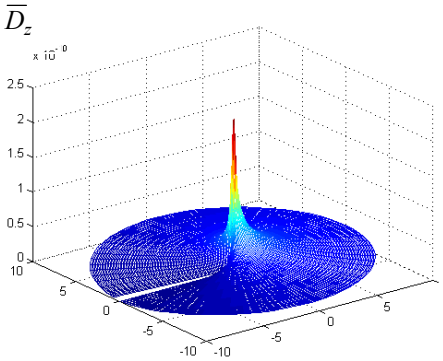

Fig. 10. Piezoelectric displacements $\overline{D}_z = \overline{D}_z(r,\varphi)$

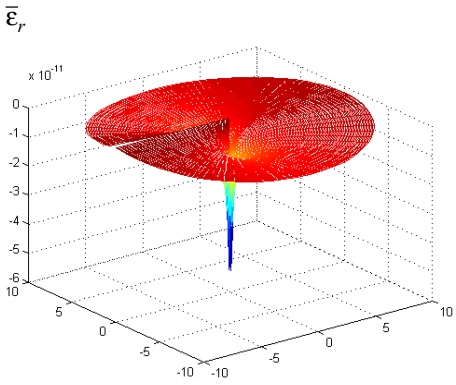

Fig. 11. Specific strain $\overline{\varepsilon}_r = \overline{\varepsilon}_r(r,\varphi)$

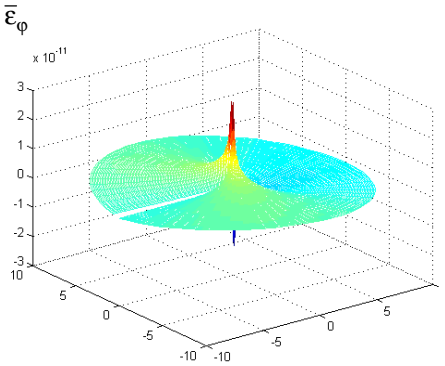

Fig. 12. Specific strain $\bar{\varepsilon}_\varphi = \bar{\varepsilon}_\varphi(r,\varphi)$

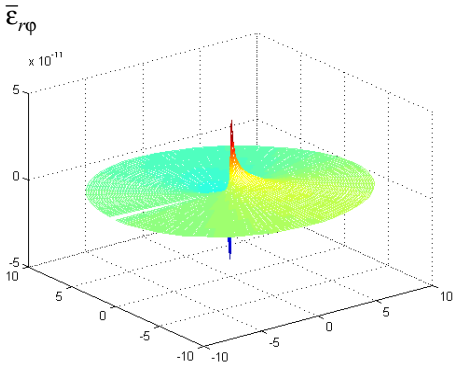

Fig. 13. Specific strain $\bar{\varepsilon}_{r\varphi} = \bar{\varepsilon}_{r\varphi}(r,\varphi)$

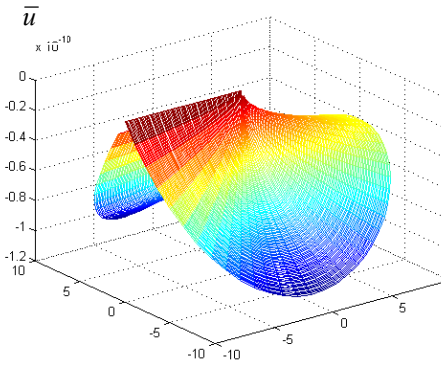

Fig. 14. Component displacement $\bar{u} = \bar{u}(r,\varphi)$

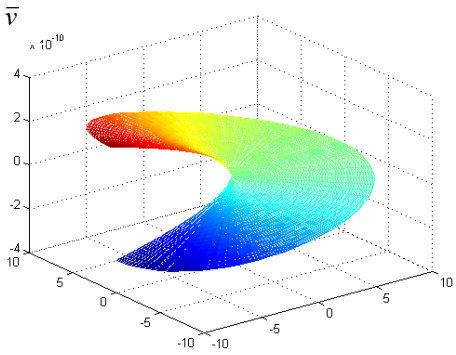

Fig. 15. Component displacement $\bar{v} = \bar{v}(r,\varphi)$

Mode II

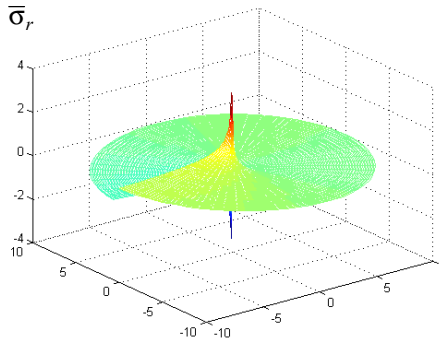

Fig. 16. Mechanical stress $\bar{\sigma}_r = \bar{\sigma}_r(r,\varphi)$

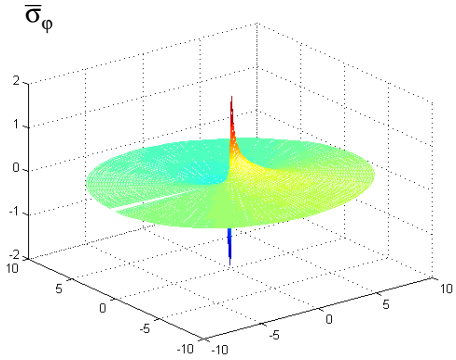

Fig. 17. Mechanical stress $\bar{\sigma}_\varphi = \bar{\sigma}_\varphi(r,\varphi)$

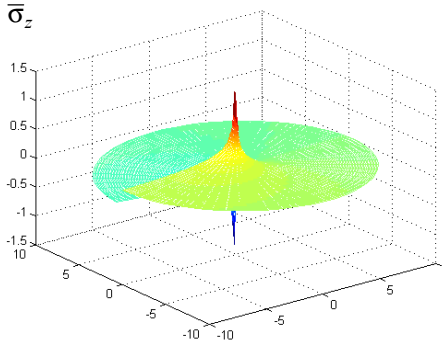

Fig. 18. Mechanical stress $\overline{\sigma}_z = \overline{\sigma}_z(r,\varphi)$

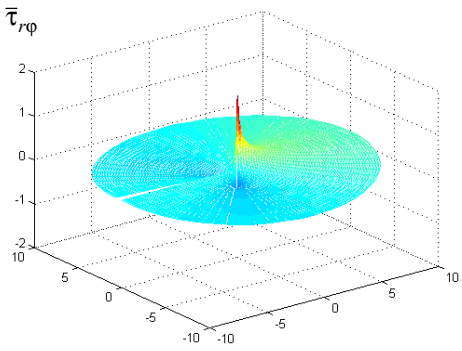

Fig. 19. Mechanical stress $\overline{\tau}_{\varphi r} = \overline{\tau}_{\varphi r}(r,\varphi)$

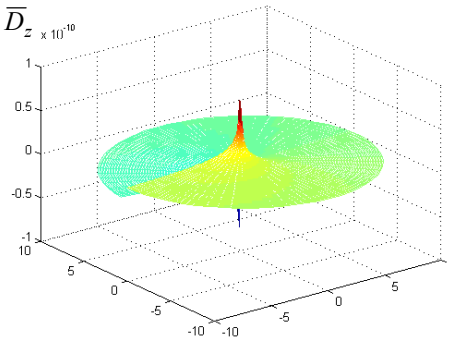

Fig. 20. Piezoelectric displacements $\overline{D}_z = \overline{D}_z(r,\varphi)$

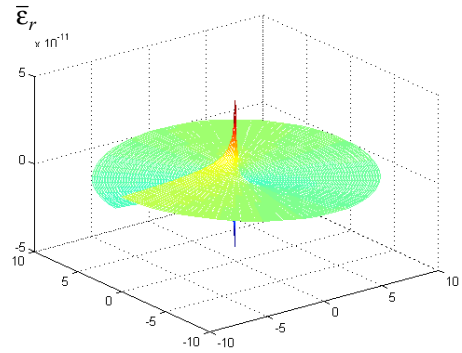

Fig. 21. Specific strain $\overline{\varepsilon}_r = \overline{\varepsilon}_r(r,\varphi)$

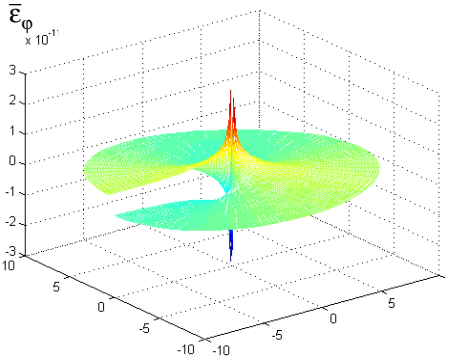

Fig. 22. Specific strain $\overline{\varepsilon}_\varphi = \overline{\varepsilon}_\varphi(r,\varphi)$

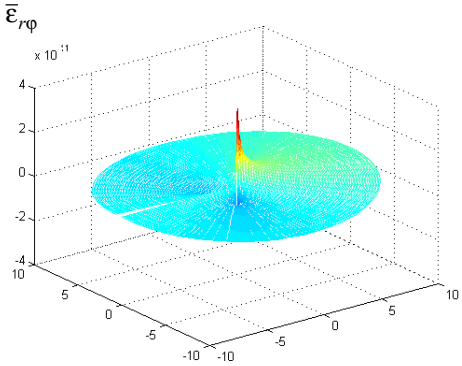

Fig. 23. Specific strain $\overline{\varepsilon}_{r\varphi} = \overline{\varepsilon}_{r\varphi}(r,\varphi)$

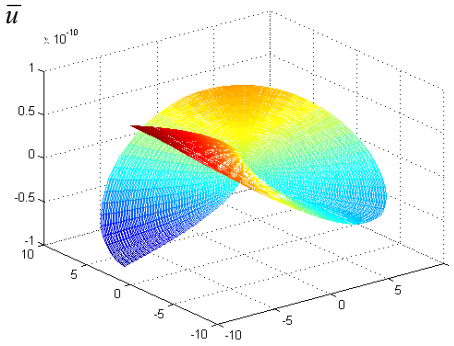

Fig. 24. Component displacement $\overline{u} = \overline{u}(r, \varphi)$

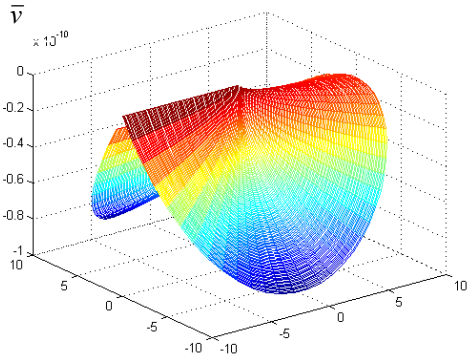

Fig. 25. Component displacement $\overline{v} = \overline{v}(r, \varphi)$

Mode III

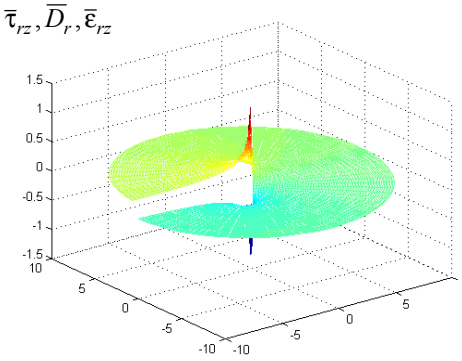

Fig. 26. Components of mechanical stress, electric displacements and specific strain $[\overline{\tau}_{rz}, \overline{D}_r, \overline{\varepsilon}_{rz}] = [\overline{\tau}_{rz}, \overline{D}_r, \overline{\varepsilon}_{rz}](r, \varphi)$

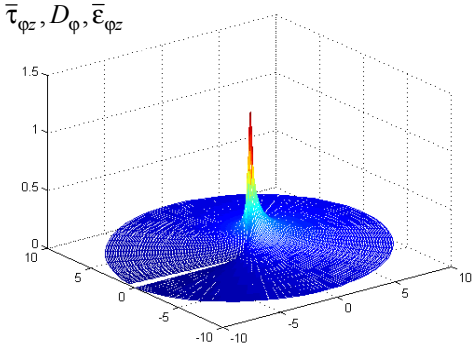

Fig. 27. Components of mechanical stress, electric displacements and specific strain $[\overline{\tau}_{\varphi z}, \overline{D}_\varphi, \overline{\varepsilon}_{\varphi z}] = [\overline{\tau}_{\varphi z}, \overline{D}_\varphi, \overline{\varepsilon}_{\varphi z}](r, \varphi)$

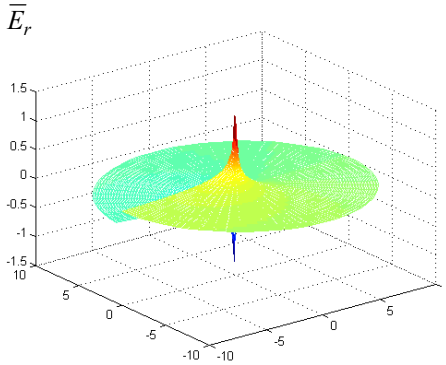

Fig. 28. Electric field $\overline{E}_r = \overline{E}_r(r, \varphi)$

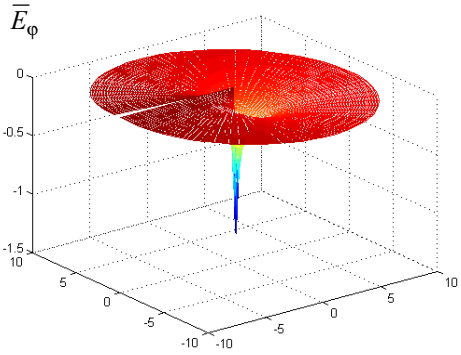

Fig. 29. Electric field $\overline{E}_\varphi = \overline{E}_\varphi(r, \varphi)$

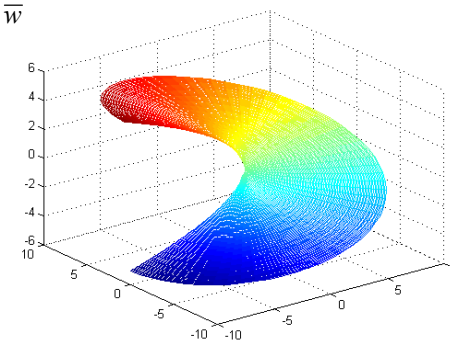

Fig. 30. Component displacement $\overline{w} = \overline{w}(r, \varphi)$

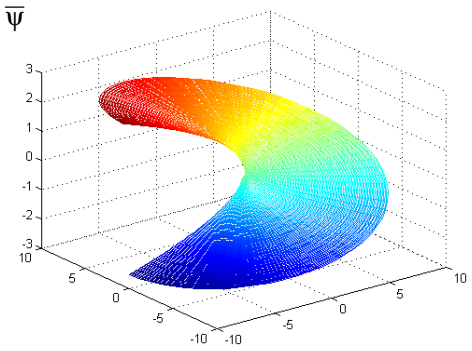

Fig. 31. Electric potential $\overline{\Psi} = \overline{\Psi}(r, \varphi)$

10. CONCLUDING REMARKS

From the analysis of the solutions of the methods presented in this work (references 6, 7, and 8), one can conclude that all methods lead to equal approximate solutions for a finite number of the members of the series (n = 0,1,2,...). However, the method of application of complex variable function (article 8) gives analytical solutions for n-members of the series, when $n \to \infty$. In the general case, these series are divergent, but for finite number of series members, a satisfactory precision can be achieved

The method of representing the components (u, v, w) of the displacement vector $\vec{s}$ by a double infinite series of arbitrary functions (article 6) is complicated and lengthy and gives solution in several steps (n = 0,1,2). Contrary, the other two methods are substantially faster. In the method of decomposition into a state of plane strain and a state of out of crack plane shear (article 7), in the first step one performs a decomposition of the spatial problem into three basic modes of crack deformation, and then an analysis of every single mode (Mode I, Mode II, Mode III) is performed. At last, when the crack front is a curve in plane, or a curve in space, summing of the results according to expressions (1) or (2), respectively, is performed.

One can see that in solutions (36)÷(66) two independent variables, the polar radius r and the polar angle φ appear. Numerical results of the analysis of obtained solutions, for all three modes of deformation are processed in MATLAB, for a polar-cylindrical system of coordinates. Thus one gets spatial diagrams of the normalized values of tensor components of mechanical stress, piezoelectric displacements, specific mechanical strain, displacement vector $\vec{s}$, electric field, and electric potential (Figure 6. ÷ Figure 31). Spatial diagrams obtained by programming in MATLAB show influence of every component on crack growth process in piezoelectric material, which represents a detailed spatial analysis of the state of previouly mentioned tensors in the vicinity of the crack tip. The influence of the values that reach their extremes on the crack surfaces, and on its front is significant, because they substantially affect the propagation (growth) of the crack in a piezoelectric material, and must not be neglected.

From figures 6 to 31 one can observe that the singularity of the components of the tensor of mechanical stress, piezoelectric displacements, relative mechanical strain, and

electric field, results from the theoretical solution only, because pure elasticity practically does not occur (ideally elastic materials). Even at small deformations of any type, a plastic zone is formed immediately around the crack tip, which makes the stress values finite. If the nonlinear area at the crack tip is so small, that it is completely contained in the field of elastic stresses, then its influence on the stress distribution at some distance from the crack front can be expressed by stress intensity factors K_I, K_{II}, K_{III}, which represent a measure of the stresses near the crack tip.

From the obtained results, one can conclude that the existence of a crack in a stressed piezoelectric material leads to a stress redistribution and concentration, and the tensors of mechanical and piezoelectric stress at the crack tip become infinitely large. The crack tip is then a point of stress singularity, and the location of the highest stress concentration. In that point the piezoelectric material is most sensitive to the subsequent occurrence of fracture.

The methods of analysis presented in this paper contribute to the methodology for analysis of the influence of the various parameters on crack growth, which helps in the design and reduces unnecessary cost of very expensive experiments.

General characteristics of the present work are summarized as:

- An analysis of the form and orientation of the crack was performed. Other forms of cracks and their orientation were not studied of this paper.
- The methods of spatial analysis presented in this work can be applied to other kinds of materials with cracks.
- These methods can be used for the analysis of the crack behavior in piezoelectric materials, as well as to control a great number of parameters, which can affect crack growth.
- An analysis is given for determining the critical size of a fault of crack type, and for other forms of crack deformation and directions of load action. These results are useful for producers and users of piezoceramic materials.
- Agreement of results obtained by different analytical methods was obtained.

The method of decomposition into plane strain state and out of plane shear, as well as the method of application of complex variable function (reference 7 and 8) represent a qualitatively new approach in research of these problems. Decomposition of the spatial stress into three components of stress for the three basic forms of crack deformation was needed not only to enable an easier approach in determining analytical solutions, but also to individually identify the influence of every component on crack propagation in piezoelectric materials. Based to such approach, analytical solutions and spatial diagrams of the state of crack deformation in piezoelectric material for all modes of deformation were obtained individually (Figures 6 to 31).

Acknowledgment. Parts of this research were supported by the Ministry of Sciences, Technologies and Development of Republic Serbia trough Mathematical Institute SANU Belgrade Grants No. 1616 *Real Problems on Mechanics* and Faculty of Mechanical Engineering University of Niš Grant No. 1828 *Dynamics and Control of Active Structures.*

REFERENCES

1. Deeg W. F. The analysis of dislocation, crack, and inclusion problems in piezoelectric solids, Ph. D. Thesis, Stanford University, 1980.
2. Freiman S. W. Mechanical behavior of ferroelectrics ceramics, IEEE Sixth Internat. Symp. On Applicat. of Ferroelectrics, pp.367-373, 1986.
3. Gdontos E.E. Fracture Mechanics, An Introduction, Kluwer Academic Publisher, pp.307, 1993.
4. Harrison W. B, McHenry K. D. Monolithic multilayer piezoelectric ceramic transducers, IEEE Sixth I. Symp. On applicat. Of Ferroelectrics, pp. 265-272, 1986.
5. Hartranft R. J, Sih G. C. The use eigenfunction expansions in the general solution of threedimensio. Crack problems, J. Math. Mech.19, 123-138, 1969.
6. Hedrih K, Perić Lj. Application of the complex variable function to crack problem in the piezelectric material, Theor. And Appl. Mec. N18, pp.41-80, Bgd. 1992.
7. Hedrih K, Perić Lj. Primena funkcije kompleksne promenljive u analizi stanja napona i stanja deformacija u piezoelektričnom materijalu sa prslinom, zb. rad. 20. Jug. kong. teor. i prim. mehan., sek. S, str. 144-147, Krag., 1993.
8. Hedrih K, Perić Lj. Stanje napona i stanje deformacija u piezoelektričnom materijalu u okolini vrha prsline za slučaj ravne deformacije, časopis Tehnika-mašinstvo, br.45, 3-4, s. M50-M56, Beograd, 1996.
9. Hedrih K, Perić Lj. Stanje napona i stanje deformacija u piezoelektričnom materijalu u okolini vrha prsline za slučaj smicanja izvan referentne ravni, časopis Tehnika-mašinstvo, br.46, 5-6, s. M11-M16, Bgd., 1997.
10. Hedrih K. Izabrana poglavlja teorije elastičnosti, Mašinski fakultet, Niš, 1988.
11. Hedrih K, Jovanović D. Matematička teorija mehanike loma i oštećenja – rečnik pojmova i prilozi, Mašinski fakultet Niš, projekt 1828, preprint.
12. Krajčinović D, Šumarac D. Osnovi mehanike loma, Naučna knjiga, Beograd, 1990.
13. Musheliśvili N.I. Same Basic Problems of the Mathematical Theory of Elasticity, P. Noordhoff Ltd., Groningen-Holland, 1953.
14. Pak E.Y. Crack extension force in a piezoelectric material, Journal of Applied Mechanics, Vol.57, pp.647-653, september 1990.
15. Pak E.Y. Force on a Piezoelectric Screw Dislocation, Journal of Applied Mechanics, Vol. 57, pp. 863-870, December 1990.
16. Parton V. Z. Fracture mechanics of piezoelectric materials, Acta Astronautica, vol. 3, pp. 671-683, 1976.
17. Perić Lj. Prostorna analiza naponskog i deformacionog stanja napregnutog piezoelektričnog materijala, Magistarska teza, c. 251, MF – Niš, 1992.
18. Pisarenko G.G, Chushko V. M. Anisotropy of fracture toughness of piezoelectric ceramics, J. Am. Ceram. Soc. 68, 259-265, 1985.
19. Sosa H. A. Pak Y. E. Three-Dimensional Eigenfunction Analysis of a Crack in a Piezoelectric material, Int. J. S. St., Vol.26, No.1, pp.1-15, 1990.
20. Westergaard H.M. Bearing pressures and crack, Journal of Applied Mechanics, Series A, Vol.66, p.49., 1939.

METODE ZA REŠAVANJE PROBLEMA NAPREZANJA ELEKTROELASTIČNIH PIEZOELEKTRIČNIH TELA SA DEFEKTIMA PRIMENOM SPECIJALNE ANALIZE I MATLABA

Katica (Stevanović) Hedrih, Ljubiša Perić

U radu je dat pregled metoda koje su primenljive za izučavanje stanja mehaničkih napona, stanja deformacija i stanja električnog polja polarizacije u okolini vrha konstruktivne prsline u ploči beskonačnih dimenzija i od piezoelektričnog materijala. Korišćenjem različitih metoda proučena su analitička rešenja, kao i grafičke vizualizacije stanja mehaničkog napona, stanja deformacije i stanja električnog polja polarizacije u tačkama u okolini vrha prsline u ploči od piezokeramičkog materijala. Korišćene su mogućnosti MATLABA.

Ključne reči: *Piezoelektrično telo, prslina, defekt, analitičke metode, stanje napona, stanje deformacija, električno polje, vizuelizacija, MATLAB.*